J|A|C|S ARTICLES

Published on Web 12/11/2008

# First-Principles Prediction of Thermodynamically Reversible Hydrogen Storage Reactions in the Li-Mg-Ca-B-H System

V. Ozolins,*,† E. H. Majzoub,§ and C. Wolverton‡

*Department of Materials Science and Engineering, University of California, Los Angeles, California 90095-1595, Department of Physics and Astronomy and Center for Nanoscience, University of Missouri, St. Louis, Missouri 63121, and Department of Materials Science and Engineering, Northwestern University, Evanston, Illinois 60208*

Received August 22, 2008; E-mail: vidvuds@ucla.edu

***Abstract:*** Introduction of economically viable hydrogen cars is hindered by the need to store large amounts of hydrogen. Metal borohydrides [$LiBH_4$, $Mg(BH_4)_2$, $Ca(BH_4)_2$] are attractive candidates for onboard storage because they contain high densities of hydrogen by weight and by volume. Using a set of recently developed theoretical first-principles methods, we predict currently unknown crystal structures and hydrogen storage reactions in the Li-Mg-Ca-B-H system. Hydrogen release from $LiBH_4$ and $Mg(BH_4)_2$ is predicted to proceed via intermediate $Li_2B_{12}H_{12}$ and $MgB_{12}H_{12}$ phases, while for Ca borohydride two competing reaction pathways (into $CaB_6$ and $CaH_2$, and into $CaB_{12}H_{12}$ and $CaH_2$) are found to have nearly equal free energies. We predict two new hydrogen storage reactions that are some of the most attractive among the presently known ones. They combine high gravimetric densities (8.4 and 7.7 wt % $H_2$) with low enthalpies [approximately 25 kJ/(mol $H_2$)] and are thermodynamically reversible at low pressures due to low vibrational entropies of the product phases containing the $[B_{12}H_{12}]^{2-}$ anion.

## I. Introduction

Since the discovery of reversible hydrogen storage in titanium-doped sodium alanate,[1] many other classes of solid-state hydrides have been investigated as candidates for on-board storage, including metal hydrides and alanates,[2,3] amides,[4,5] and amino boranes.[6−9] Recently, attention has shifted to borohydrides, which have some of the highest hydrogen densities by weight and by volume.[10−17] Since many borohydrides suffer from the drawback of very strongly bound hydrogen, Vajo et al.[18] generated enormous interest by demonstrating "destabilization" in the $LiBH_4-MgH_2$ system, which uses phase formation of $MgB_2$ to significantly decrease the temperature of hydrogen release relative to pure $LiBH_4$. Since then, numerous other destabilized reactions involving borohydrides have been predicted theoretically[19−23] and tested experimentally.[24−26] It is commonly assumed that the decomposition products of destabilized borohydride reactions are binary metal borides and/or hydrides;[27] under these assumptions, several of the predicted new reactions are calculated to have thermodynamic properties that approach the desired window for reversible on-board storage. Recent studies, however, question this accepted view:

† University of California, Los Angeles.
§ University of Missouri, St. Louis.
‡ Northwestern University.

(1) Bogdanovic, B.; Schwickardi, M. *J. Alloys Compd.* **1997**, *253*, 1–9.
(2) Sandrock, G. *J. Alloys Compd.* **1999**, *293*, 877–888.
(3) Sandrock, G.; Reilly, J.; Graetz, J.; Zhou, W.-M.; Johnson, J.; Wegrzyn, J. *Appl. Phys. A: Mater. Sci. Process.* **2005**, *80*, 687–690.
(4) Chen, P.; Xiong, Z.; Luo, J.; Lin, J.; Tan, K. L. *Nature* **2002**, *420*, 302–304.
(5) Luo, W. *J. Alloys Compd.* **2004**, *381*, 284–287.
(6) Wolf, G.; Baumann, J.; Baitalow, F.; Hoffmann, F. P. *Thermochim. Acta* **2000**, *343*, 19–25.
(7) Stowe, A. C.; Shaw, W. J.; Linehan, J. C.; Schmid, B.; Autrey, T. *Phys. Chem. Chem. Phys.* **2007**, *9*, 1831–1836.
(8) Miranda, C.; Ceder, G. *J. Chem. Phys.* **2007**, *126*, 184703.
(9) Xiong, Z.; Yong, C. K.; Wu, G.; Chen, P.; Shaw, W.; Karkamkar, A.; Autrey, T.; Jones, M. O.; Johnson, S. R.; Edwards, P. P.; David, W. I. F. *Nat. Mater.* **2008**, *7*, 138–141.
(10) Zuttel, A.; Wenger, P.; Rentsch, S.; Sudan, P.; Mauron, P.; Emmenegger, C. *J. Power Sources* **2003**, *118*, 1–7.
(11) Miwa, K.; Aoki, M.; Noritake, T.; Ohba, N.; Nakamori, Y.; Towata, S.; Zuttel, A.; Orimo, S. *Phys. Rev. B* **2006**, *74*, 155122.
(12) Vajeeston, P.; Ravindran, P.; Kjekshus, A.; Fjellvag, H. *Appl. Phys. Lett.* **2006**, *89*, 071906.
(13) Nakamori, Y.; Miwa, K.; Ninomiya, A.; Li, H. W.; Ohba, N.; Towata, S. I.; Zuttel, A.; Orimo, S. I. *Phys. Rev. B* **2006**, *74*, 045126.
(14) Cerny, R.; Filinchuk, Y.; Hagemann, H.; Yvon, K. *Angew. Chem., Int. Ed.* **2007**, *46*, 5765–5767.
(15) Her, J. H.; Stephens, P. W.; Gao, Y.; Soloveichik, G. L.; Rijssenbeek, J.; Andrus, M.; Zhao, J. C. *Acta Crystallogr. B* **2007**, *63*, 561–568.
(16) Chlopek, K.; Frommen, C.; Leon, A.; Zabara, O.; Fichtner, M. *J. Mater. Chem.* **2007**, *17*, 3496–3503.
(17) Kolmogorov, A. N.; Drautz, R.; Pettifor, D. G. *Phys. Rev. B* **2007**, *76*, 184102.
(18) Vajo, J. J.; Skeith, S. L.; Mertens, F. *J. Phys. Chem. B* **2005**, *109*, 3719–3722.
(19) Alapati, S. V.; Johnson, J. K.; Sholl, D. S. *J. Phys. Chem. B* **2006**, *110*, 8769–8776.
(20) Alapati, S. V.; Johnson, J. K.; Sholl, D. S. *J. Alloys Compd.* **2007**, *446*, 23–27.
(21) Alapati, S. V.; Johnson, J. K.; Sholl, D. S. *Phys. Rev. B* **2007**, *76*, 104108.
(22) Alapati, S. V.; Johnson, J. K.; Sholl, D. S. *J. Phys. Chem. C* **2008**, *112*, 5258–5262.
(23) Siegel, D.; Wolverton, C.; Ozolins, V. *Phys. Rev. B* **2007**, *76*, 134102.
(24) Yang, J.; Sudik, A.; Wolverton, C. *J. Phys. Chem. C* **2007**, *111*, 19134–19140.
(25) Pinkerton, F. E.; Meyer, M. S.; Meisner, G. P.; Balogh, M. P.; Vajo, J. J. *J. Phys. Chem. C* **2007**, *111*, 12881–12885.
(26) Purewal, J.; Hwang, S.-J.; Bowman, R. C.; Ronnebro, E.; Fultz, B.; Ahn, C. C. *J. Phys. Chem. C* **2008**, *112*, 8481–8485.
(27) Vajo, J. J.; Salguero, T. T.; Gross, A. E.; Skeith, S. L.; Olson, G. L. *J. Alloys Compd.* **2007**, *446*, 409–414.


10.1021/ja8066429 CCC: $40.75 

Some authors surprisingly find that icosahedral $Li_2B_{12}H_{12}$ and $MgB_{12}H_{12}$ phases may be stable intermediates in the decomposition sequences of $LiBH_4$ and $Mg(BH_4)_2$, respectively.[28−32] The crystal structures of these compounds are currently not known, and the thermodynamics of these reactions are poorly understood. Therefore, the true potential of borohydrides for hydrogen storage remains unsettled.

We have recently developed a comprehensive array of first-principles density functional theory (DFT)-based methods aimed at theoretically predicting the structural and thermodynamic properties of multicomponent complex hydrides. Two techniques are of particular importance: (1) the prototype electrostatic ground state (PEGS) search method[32,33] to predict unknown crystal structures of complex hydrides, and (2) the DFT-based linear programming approach[34] to elucidate the thermodynamically preferred (but often chemically non-intuitive) $H_2$ release pathways that can occur in multicomponent hydrides. Previously, we have applied each of these techniques *separately* to a variety of hydrogen storage systems. Here, using borohydrides in the Li-Ca-Mg-B-H system as an example, we show how the *combination* of these two methods provides a powerful theoretical framework for predicting new high-capacity hydrogen storage reactions with excellent thermodynamic properties. In particular, we use PEGS to predict the currently unknown crystal structures of $X_nB_{12}H_{12}$ compounds, where X = Li, Mg, or Ca, and combine the predicted thermodynamics of these new phases with the linear programming approach to determine thermodynamically favored reaction pathways and predict new $H_2$ storage reactions. We find that $LiBH_4$ and $Mg(BH_4)_2$ are thermodynamically favored to release $H_2$ by forming $Li_2B_{12}H_{12}$ and $MgB_{12}H_{12}$, respectively, while $Ca(BH_4)_2$ has two thermodynamically degenerate decomposition pathways, one of which involves an intermediate $CaB_{12}H_{12}$ phase, while the other goes directly to $CaB_6$ and $CaH_2$. Surprisingly, we also find that the classical destabilized $LiBH_4 + MgH_2$ reaction[18] is thermodynamically favored to proceed via an intermediate $Li_2B_{12}H_{12}$ compound. Most importantly, we find two new, previously unsuspected reactions involving the predicted $Li_2B_{12}H_{12}$ and $CaB_{12}H_{12}$ phases as reaction products. These reactions have some of the most attractive thermodynamic properties and storage densities among the currently known solid-state hydrogen storage systems. More broadly, our work demonstrates that first-principles theoretical design of new materials for energy storage is now possible, paving the way for similar studies in the future.

## II. Methods

**A. First-Principles Free Energy Calculations.** The first-principles DFT method of electronic structure calculations was used to calculate the total binding energies of all the compounds studied here. The electronic exchange correlation was treated within the generalized gradient approximation (GGA) of Perdew and Wang,[35] and the projected augmented wave (PAW) approach, as implemented in the *ab initio* total-energy and molecular dynamics code VASP,[35−39] was used to treat the interactions between the nuclei and valence electrons. The plane wave basis set for the electronic wave functions was defined by a cutoff energy of 875 eV, and the Brillouin zones of solid phases were sampled using 4 × 4 × 4 Monkhorst−Pack *k*-point meshes. Structural relaxations of atomic positions, cell shapes, and cell volumes were carried out until the residual forces and stresses were less than 0.01 eV/Å and 0.1 GPa, respectively. The energy of the $H_2$ molecule was calculated by placing the molecule in a 10 × 10 × 12 Å rectangular box. The phonon frequencies were determined using the dynamical matrix approach where all symmetry-inequivalent rows of the dynamical matrix were calculated by displacing the ions for a total of five 0.03 Å steps around their equilibrium positions. The vibrational entropies and enthalpies were obtained by summing over the normal-mode frequencies.

**B. Crystal Structure Search.** We used the recently developed PEGS search method to predict the unknown ground-state crystal structures of $X_nB_{12}H_{12}$ compounds.[33] Physically, this approach is based on the observation that most of the known complex hydride compounds are characterized by an arrangement of positively charged cations (e.g., $Li^+$, $Mg^{2+}$, and $Ca^{2+}$) and negatively charged anions (e.g., $[BH_4]^-$ or $[B_{12}H_{12}]^{2-}$) with strong electrostatic interactions between the ions.[40] The premise of the PEGS method is that the topology and symmetry of the ground-state crystal structure can be determined by minimizing the total electrostatic energy using fixed shapes of complex anions and soft-sphere repulsion between the ions. The resulting structures are then fully relaxed using first-principles DFT calculations to obtain accurate total energies and structural parameters. The PEGS Hamiltonian includes electrostatic and soft-core interionic repulsion terms:

$$H_{\mathrm{PEGS}} = \sum_{i<j} \left( \frac{Z_i Z_j}{r_{ij}} + \frac{1}{r_{ij}^{12}} \right) \tag{1}$$

where the sums run over all ions, $r_{ij}$ is the separation between ions $i$ and $j$, $Z_i$ is the ionic charge, and the second term (soft-core repulsion) is zero for non-overlapping ions. Monte Carlo-simulated annealing, in conjunction with distance scaling potential energy surface smoothing techniques,[41] is used to minimize the electrostatic energy. The PEGS method bears distant resemblance to the automated assembly of secondary building units (AASBU) method.[42] However, the structure of complex ions is more detailed in PEGS than in AASBU, and simple physical interactions are used in PEGS, while special rules are created for the AASBU interactions, such as "sticky" spots on the building units.

To expedite the Monte Carlo minimization and because the external atoms of the anion are dominant in the Hamiltonian, the $[B_{12}H_{12}]^{2-}$ anion was modeled as a rigid unit with hydrogen atoms at icosahedral vertex positions 2.95 Å from the geometric center. A hydrogen radius of 1.43 Å was chosen from the DFT-relaxed Mg−H distance in a trial structure for $MgB_{12}H_{12}$. The total ionic charge of $-2e$ was distributed equally among the vertex hydrogen ions. Boron atoms were added after the Monte Carlo minimization at a distance of 1.12 Å inward from the H ions. For each compound approximately 15−30 structures were run in parallel for several

(28) Ohba, N.; Miwa, K.; Aoki, M.; Noritake, T.; Towata, S.; Nakamori, Y.; Orimo, S.; Züttel, A. *Phys. Rev. B* **2006**, *74*, 075110.
(29) Li, H.-W.; Kikuchi, K.; Nakamori, Y.; Ohba, N.; Miwa, K.; Towata, S.; Orimoa, S. *Acta Mater.* **2008**, *56*, 1342–1347.
(30) Soloveichik, G. L.; Gao, Y.; Rijssenbeek, J.; Andrus, M.; Kniajanski, S.; Bowman, R. C.; Hwang, S.-J.; Zhao, J. C. Unpublished, 2008.
(31) Hwang, S.-J.; Bowman, R. C.; Reiter, J. W.; Rijssenbeek, J.; Soloveichik, G. L.; Zhao, J. C.; Kabbour, H.; Ahn, C. C. *J. Phys. Chem. C* **2008**, *112*, 3164–3169.
(32) Ozolins, V.; Majzoub, E. H.; Wolverton, C. *Phys. Rev. Lett.* **2008**, *100*, 135501.
(33) Majzoub, E. H.; Ozolins, V. *Phys. Rev. B* **2008**, *77*, 104115.
(34) Akbarzadeh, A.; Ozolins, V.; Wolverton, C. *Adv. Mater.* **2007**, *19*, 3233–3239.
(35) Perdew, J. P.; Wang, Y. *Phys. Rev. B* **1992**, *45*, 13244–13249.
(36) Blochl, P. E. *Phys. Rev. B* **1994**, *50*, 17953–17979.
(37) Kresse, G.; Furthmüller, J. *Comput. Mater. Sci.* **1996**, *6*, 15–50.
(38) Kresse, G.; Furthmüller, J. *Phys. Rev. B* **1996**, *54*, 11169–11186.
(39) Kresse, G.; Joubert, D. *Phys. Rev. B* **1999**, *59*, 1758–1775.
(40) Ozolins, V.; Majzoub, E. H.; Udovic, T. *J. Alloys Compd.* **2004**, *375*, 1–10.
(41) Wawak, R. J.; Pillardy, J.; Liwo, A.; Gibson, K. D.; Scheraga, H. A. *J. Phys. Chem. A* **1998**, *102*, 2904–2918.
(42) Mellot-Draznieks, C.; Férey, G. *Prog. Solid State Chem.* **2005**, *33*, 187–197.

***Table 1.*** Lowest-Energy $X_nB_{12}H_{12}$ Structures Found by the PEGS Search

| compd | symmetry | Pearson symbol |
|---|---|---|
| $Li_2B_{12}H_{12}$ | *C*2/*m* (space group 12) | mC52 |
| $MgB_{12}H_{12}$ | *C*2/*m* (space group 12) | mC50 |
| $CaB_{12}H_{12}$ | *C*2/*c* (space group 15) | mC100 |

different values of a starting random number seed, which initializes the cell contents. The final post-DFT relaxed energies were then used to select the global ground state.

**C. Determining Hydrogen Release Reactions.** The grand canonical linear programming method of ref 34 was used to determine thermodynamically reversible hydrogen storage reactions. Consider a multiphase solid containing a certain fixed ratio of non-hydrogen species, which can exchange hydrogen with a reservoir of $H_2$ gas at a chemical potential $\mu_{H_2}(p,T)$; the latter is a function of temperature $T$ and pressure $p$. The grand-canonical Gibbs free energy is given by the following expression:

$$\Xi(p,T) = \sum_i x_i F_i(T) - \frac{\mu_{H_2}(p,T)}{2} \sum_i x_i n_i^H \qquad (2)$$

where $F_i(T)$ is the free energy of phase $i$ (we neglect the pressure dependence of the free energies of solid phases), $n_i^H$ is the number of hydrogen ions in one formula unit of phase $i$, and $x_i$ are the unknown variable molar fractions of phases coexisting at a given composition, temperature, and pressure. The molar fractions are determined by minimizing eq 2, subject to the mass-conservation constraints for non-hydrogen species:

$$f_s = \sum_i x_i n_i^s = \text{const for } \forall\, s \neq H \qquad (3)$$

where $n_i^s$ is the number of ions of type $s$ in one formula unit of phase $i$, and $f_s$ represents given molar ratios of the non-hydrogen species (i.e., Li, Mg, Ca, and B); the latter are normalized to obey $\sum_{s\neq H} f_s = 1$. Equations 2 and 3 constitute a linear programming problem, where the unknown variables are molar fractions of the possible phases, $x_i$. To obtain $x_i$ as functions of composition, pressure, and temperature, we minimize eq 2 for a decreasing sequence of hydrogen chemical potentials $\mu_{H_2}(p,T)$, starting from $T = 0$ K, where $\mu_{H_2}$ is given by the total energy of an $H_2$ molecule. Reactions are identified by comparing the computed molar fractions at two successive values of the chemical potential; the reactants and reaction products are found as the difference between the two sets of $x_i$. The following phases were included in our study: molecular $H_2$ and bulk solids $Ca(BH_4)_2$, $CaB_{12}H_{12}$, $CaH_2$, $CaB_6$, $MgB_2H_8$, $MgB_{12}H_{12}$, $MgH_2$, $MgB_2$, $MgB_4$, $MgB_7$, $LiBH_4$, $Li_2B_{12}H_{12}$, LiH, Ca, Li, Mg, and B.

## III. Results

**A. Crystal Structures of $X_nB_{12}H_{12}$ Compounds.** Determining the crystal structures of all stable compounds in the Li-Mg-Ca-B-H system is the first step required by our approach. Knowledge of the crystal structures allows us to compute the thermodynamics of all phases from first-principles DFT and subsequently use this input into the linear programming method to predict new high-capacity hydrogen storage reactions.

In addition to studying compounds with known crystal structures (see section II.C), we focus our attention on predicting the currently unknown crystal structures of compounds involving an icosahedral $[B_{12}H_{12}]^{2-}$ complex. We note that boron−hydrogen chemistry allows for a rich family of possible bonding topologies, such as $[B_3H_8]^-$, $[B_6H_6]^{2-}$, $[B_{10}H_{10}]^{2-}$, and others. Our focus on the $X_nB_{12}H_{12}$ compounds is motivated by recent

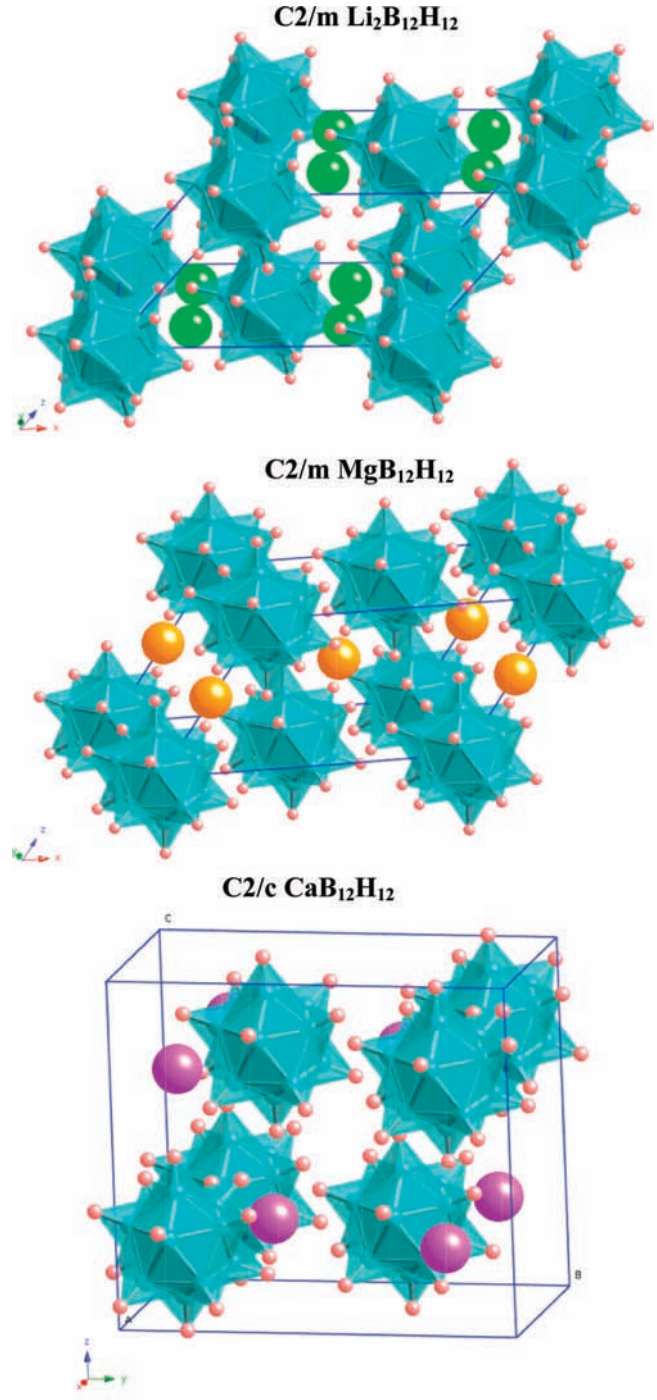


***Figure 1.*** Predicted crystal structures of $X_nB_{12}H_{12}$ compounds.

experimental results[29−31] pointing to the formation of these compounds during hydrogen release from borohydrides and by a prior DFT study,[28] which considered various $LiB_3H_8$ and $Li_mB_nH_n$ compounds and found that $Li_2B_{12}H_{12}$ is the only stable intermediate in the decomposition sequence of $LiBH_4$. Using PEGS,[33] we conducted ground-state crystal structure searches using one- and two-formula unit primitive cells for $Li_2B_{12}H_{12}$, $MgB_{12}H_{12}$, and $CaB_{12}H_{12}$ (see section II.B). The lowest-energy structures found in this search are listed in Table 1, giving their symmetries and Pearson symbols, and shown graphically in Figure 1. The DFT-relaxed lattice parameters, cell angles, atomic coordinates, and near-neighbor coordination data are given in the Supporting Information. For $Li_2B_{12}H_{12}$, our structure is ∼7

***Table 2.*** Predicted Decomposition Reactions for Borohydrides[a]

| | reaction | wt % (kg $H_2$/kg) | vol density (g $H_2$/l) | $\Delta H^{0\ K}$ | $\Delta H^{300\ K}$ | $\Delta S^{300\ K}$ | $T_c$ (°C) |
|---|---|---|---|---|---|---|---|
| | Decomposition of Pure $X_nB_{12}H_{12}$Compounds | | | | | | |
| (1) | $Li_2B_{12}H_{12} \rightarrow 2LiH + 12B + 5H_2$ | 6.5 | 60 | 109.4 | 116.7 | 120.4 | 696 |
| (2) | $MgB_{12}H_{12} \rightarrow MgB_7 + 5B + 6H_2$ | 7.3 | 72 | 62.8 | 71.5 | 122.8 | 309 |
| (3) | $CaB_{12}H_{12} \rightarrow CaB_6 + 6B + 6H_2$ | 6.7 | 84 | 65.0 | 73.7 | 127.4 | 306 |
| | Destabilized Reactions with $X_nB_{12}H_{12}$ Compounds | | | | | | |
| (4) | $Li_2B_{12}H_{12} + 2CaH_2 \rightarrow 2CaB_6 + 2LiH + 7H_2$ | 5.9 | 67 | 43.1 | 51.1 | 128.2 | 123 |
| (5) | $Li_2B_{12}H_{12} + 6Mg \rightarrow 6MgB_2 + 2LiH + 5H_2$ | 3.3 | 40 | 53.4 | 60.2 | 112.0 | 259 |
| (6*) | $Li_2B_{12}H_{12} + 6MgH_2 \rightarrow 6MgB_2 + 2LiH + 11H_2$ | 7.1 | 53 | 52.4 | 60.1 | 123.3 | 215 |
| (7) | $MgB_{12}H_{12} + 5MgH_2 \rightarrow 6MgB_2 + 11H_2$ | 7.5 | 86 | 42.1 | 50.0 | 123.9 | 128 |
| (8) | $CaB_{12}H_{12} + CaH_2 \rightarrow 2CaB_6 + 7H_2$ | 6.3 | 85 | 38.6 | 47.0 | 130.7 | 86 |
| (9) | $CaB_{12}H_{12} + 3MgH_2 \rightarrow 3MgB_2 + CaB_6 + 9H_2$ | 7.0 | 91 | 45.2 | 53.2 | 126.7 | 144 |
| | Decomposition of $LiBH_4$ | | | | | | |
| (10) | $12LiBH_4 \rightarrow Li_2B_{12}H_{12} + 10LiH + 13H_2$ | 10.0 | 35 | 40.9 | 44.4 | 97.4 | 171 |
| (11*) | $LiBH_4 \rightarrow LiH + B + (3/2)H_2$ | 13.8 | 95 | 60.0 | 64.5 | 103.7 | 350 |
| | Decomposition of $Mg(BH_4)_2$ | | | | | | |
| (12) | $6Mg(BH_4)_2 \rightarrow MgB_{12}H_{12} + 5MgH_2 + 13H_2$ | 8.1 | 46 (63) | 25.0 | 29.3 | 99.8 | 20 |
| (13*) | $Mg(BH_4)_2 \rightarrow MgB_2 + 4H_2$ | 14.9 | 80 (117) | 32.8 | 38.8 | 111.6 | 75 |
| | Decomposition of $Ca(BH_4)_2$ | | | | | | |
| (14) | $6Ca(BH_4)_2 \rightarrow CaB_{12}H_{12} + 5CaH_2 + 13H_2$ | 6.3 | 68 | 34.2 | 39.2 | 106.5 | 99 |
| (15) | $3Ca(BH_4)_2 \rightarrow CaB_6 + 2CaH_2 + 10H_2$ | 9.6 | 105 | 35.2 | 40.8 | 111.3 | 94 |
| | Decomposition of $MgH_2$ | | | | | | |
| (16) | $MgH_2 \rightarrow Mg + H_2$ | 7.7 | 110 | 52.0 | 60.3 | 132.1 | 181 |
| | Known Destabilized Reactions with $LiBH_4$ | | | | | | |
| (17*) | $2LiBH_4 + MgH_2 \rightarrow 2LiH + MgB_2 + 4H_2$ | 11.6 | 99 | 45.7 | 51.1 | 109.2 | 195 |
| (18) | $6LiBH_4 + CaH_2 \rightarrow 6LiH + CaB_6 + 10H_2$ | 11.7 | 95 | 41.3 | 46.3 | 108.4 | 154 |
| | New Destabilized Reactions with $X(BH_4)_n$ Compounds | | | | | | |
| (19) | $5Mg(BH_4)_2 + 2LiBH_4 \rightarrow Li_2B_{12}H_{12} + 5MgH_2 + 13H_2$ | 8.4 | 46 (64) | 20.1 | 24.4 | 100.0 | −29 |
| (20) | $5Mg(BH_4)_2 + CaBH_4 \rightarrow CaB_{12}H_{12} + 5MgH_2 + 13H_2$ | 7.7 | 51 (70) | 21.3 | 25.7 | 100.5 | −18 |
| (21) | $5Ca(BH_4)_2 + 2LiBH_4 \rightarrow Li_2B_{12}H_{12} + 5CaH_2 + 13H_2$ | 6.7 | 69 | 33.0 | 37.9 | 106.0 | 83 |

[a] Enthalpies and entropies are given in kJ/(mol $H_2$) and J/(K mol $H_2$), respectively. $\Delta H^{0\ K}$ and $\Delta H^{300\ K}$ are the calculated enthalpies at $T = 0$ and 300 K, including vibrational energies. $T_c$ gives the calculated temperatures of hydrogen release at $p = 1$ bar of hydrogen pressure. Volumetric densities are obtained using the calculated ground-state lattice parameters of products; the values for reactions with $Mg(BH_4)_2$ are given for $I\bar{4}m_2$ ($P6_1$) phases.[14,15,32] Reactions marked by an asterisk are not in the thermodynamically favored decomposition sequence because they violate the thermodynamic guidelines outlined in ref 23.

kJ/mol (or ∼70 meV per formula unit) lower than the $P2_1/n$ structure proposed by Ohba et al.,[28] which was obtained by considering only two candidate $Li_2B_{12}H_{12}$ structures from the Inorganic Crystal Structure Database (ICSD). Solution-phase synthesized crystals of $Li_2B_{12}H_{12}$ have been obtained previously;[43] however, the measured X-ray diffraction patterns contain unidentified peaks due to impurity phases, making conclusive symmetry assignment an unsolved problem. Future experiments are necessary to more clearly elucidate the crystal structure of $Li_2B_{12}H_{12}$ and test our theoretical prediction. There are no existing theoretical predictions or experimental data for the crystal structures of $MgB_{12}H_{12}$ and $CaB_{12}H_{12}$, and our work constitutes the first available study of the crystal structures and thermodynamics of these compounds. All the monoclinic structures found here have no known prototypes in the ICSD and represent completely new structure types that could not have been predicted using methods based on database searching.[12,28,44] As a word of caution, we note that many borohydrides are known to exhibit structural polymorphism and high-temperature entropically stabilized phases. Our results should provide highly accurate reaction enthalpies also in these cases, since the predicted PEGS energetics are expected to be close to those of the structural polymorphs. For instance, we found that the predicted PEGS $I\bar{4}m_2$ structure of $Mg(BH_4)_2$ is 5 kJ/mol lower in energy than the solution-synthesized $P6_1$ room-temperature phase;[32] the corresponding effect on the reaction enthalpy is negligible (less than 2 kJ/mol $H_2$).

**B. Reaction Thermodynamics: Enthalpies and Entropies.** Armed with the first-principles thermodynamics of the predicted crystal $X_nB_{12}H_{12}$ phases and the other known borohydrides, borides, hydrides, and metals, we use the DFT linear programming approach[34] to identify all thermodynamically favored reactions in the quinary Li-Mg-Ca-B-H system (see Methods). The calculated thermodynamic properties of these reactions are given in Table 2. For reference, we also list several reactions that are commonly discussed in the literature but are found to be thermodynamically unrealistic because they either proceed as multistep reactions or involve unstable products or reactants;[23] these reactions are marked by an asterisk.

It can be seen that several reactions in Table 2 have enthalpies within the window of 20−45 kJ/(mol $H_2$) that is usually targeted for reversible on-board storage. Surprisingly, several of these reactions with apparently "good" enthalpies [in particular, reactions (10), (14), (15), (18), and (21)] release hydrogen above the upper limit of $T = 80$ °C set by the operating temperature of proton exchange membrane (PEM) fuel cells, indicating that the *entropies* play an important role and must be taken into account. Indeed, the 20−45 kJ/(mol $H_2$) range of enthalpies is derived from the famous van't Hoff equation, which relates the pressure and temperature of hydrogen release, $\ln(p) = (-\Delta H/RT) + (\Delta S/R)$, where $\Delta H$

(43) Johnson, J. W.; Brody, J. F. *J. Electrochem. Soc.* **1982**, *129*, 2213–2219.
(44) Fischer, C. K.; Tibetts, D.; Morgan, G. *Nat. Mater.* **2006**, *5*, 641–646.

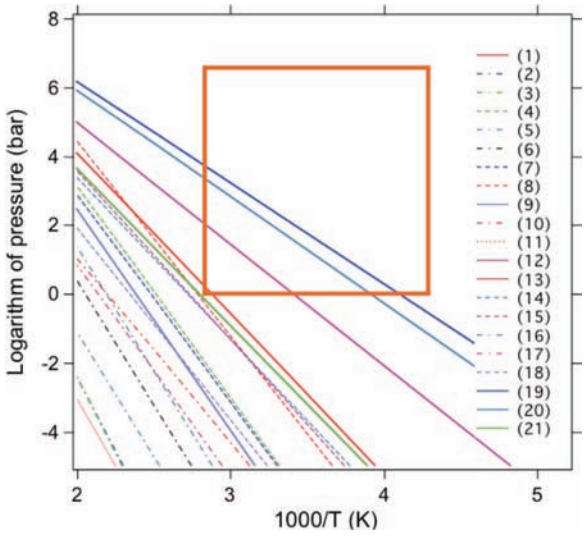


***Figure 2.*** Calculated van't Hoff plot for reactions listed in Table 2. The region within the rectangular box corresponds to desirable temperatures and pressures for on-board hydrogen storage: $p_{H_2} = 1-700$ bar and $T = -40$ to $+80$ °C.

and $\Delta S$ are the enthalpy and entropy of the dehydriding reaction, respectively. According to this equation, there is a linear relationship between $\ln(p)$ and $1/T$, where the slope is given by the reaction enthalpy and the intercept is determined by the reaction entropy. Figure 2 shows these relations (the so-called van't Hoff diagrams) for all reactions from Table 2. Assuming that $\Delta S$ is dominated by the entropy of $H_2$ gas [$\Delta S^0 = 130.68$ J/(K mol $H_2$) at $T = 20$ °C and $p = 1$ bar],[45] requiring hydrogen release at ambient pressures below 80 °C leads to the upper enthalpy limit of ~45 kJ/(mol $H_2$), while requiring rehydrogenation at a pressure of a few hundred bar or less gives the lower enthalpy limit of ~20 kJ/(mol $H_2$). However, if the reaction entropy is lower than the standard-state entropy of $H_2$ gas, *then the targeted range of enthalpies also becomes lower*. All of the aforementioned "seemingly good" reactions have entropies near 100 J/(K mol $H_2$), ~25% below the standard-state entropy of gaseous hydrogen, releasing hydrogen at temperatures that are substantially higher than those expected from purely enthalpic considerations.

Low *entropies* can also have a highly beneficial effect since they will allow the use of materials with lower reaction *enthalpies* while maintaining the same equilibrium $H_2$ pressure. Other things being equal, lower enthalpy reactions are always better due to a smaller amount of heat released during exothermic regeneration of these hydrides. We will show that our predicted reactions have the advantages of not only high capacities and excellent thermodynamic $H_2$ release temperatures but also low entropies and low enthalpies. Formation of the new $X_nB_{12}H_{12}$ compounds is found to be particularly interesting, since all of the reactions that involve them as end products [i.e., reactions (10), (12), (14), (19), (20), and (21)] have low entropies of approximately 100 J/(K mol $H_2$). This implies that the entropy (per atom) of the $[B_{12}H_{12}]^{2-}$ anion is significantly lower than the entropy of the $[BH_4]^-$ anion, which can be rationalized by counting the number of low-frequency vibrational modes. Indeed, each cation gives rise to three translational branches, while each complex anion creates three translational and three rotational low-frequency phonon branches. Taking the decomposition reaction (12) as an example, this amounts to a significant decrease in the number of low-frequency branches from $6 \times (3 + 2 \times 6) = 90$ in $6Mg(BH_4)_2$ to $3 + 6 = 9$ and $5 \times 3 = 15$ in $MgB_{12}H_{12}$ and $5MgH_2$, respectively. These considerations suggest a rule of thumb for designing new complex hydride reactions with *low entropies*: use reactants that have complex anions constituted by a small number of atoms (such as $NH_2$, $BH_4$, etc., resulting in a high number of low-frequency phonon modes per atom) and products that are either tightly bound bulk phases or materials with large complex anions (e.g., $B_{12}H_{12}$), exhibiting few low-frequency phonon branches.

**C. Reaction Pathways. $X_nB_{12}H_{12}$ Compounds.** We begin our discussion of thermodynamically favored reaction pathways by discussing the thermodynamic properties of the newly predicted $X_nB_{12}H_{12}$ compounds. Table 2 shows that phase-pure $X_nB_{12}H_{12}$ hydrides are predicted to be extremely stable, decomposing according to reactions (1)−(3) at temperatures of several hundred degrees Celsius.

**Destabilized Reactions Involving $X_nB_{12}H_{12}$ Compounds.** Following the destabilization ideas of Reilly and Wiswall,[46,47] the hydrogen release temperatures from $X_nB_{12}H_{12}$ can be lowered significantly by forming strongly bound boride product phases; see reactions (4)−(9) in Table 2. In particular, $Li_2B_{12}H_{12}$ can be efficiently destabilized by mixing with $CaH_2$ in a 1:2 molar ratio; the resulting decomposition reaction (4) releases hydrogen at 123 °C, a dramatic decrease from the almost 700 °C decomposition temperature of pure $Li_2B_{12}H_{12}$. Another destabilization pathway for $Li_2B_{12}H_{12}$ involves the formation of the $MgB_2$ compound according to reaction (5) or (6*); these pathways are relevant for our subsequent discussion of the classical $LiBH_4 + MgH_2$ reaction.[18] We note here that our calculations predict that reaction (5) is thermodynamically reasonable, but (6*) is not, since $MgH_2$ on the left side of reaction (6*) should decompose first, at 181 °C; see reaction (16) in Table 2. However, caution should be used when comparing the thermodynamics of reactions (5) and (6*). Our predicted ambient-pressure desorption temperature for $MgH_2$ is much below typical experimentally observed values of $T_c$ ~300 °C due to a well-known tendency of the GGA[35] to underestimate the formation enthalpy of $MgH_2$. We calculate a value of 60.3 kJ/(mol $H_2$) at 20 °C, in good agreement with other theoretical DFT results[23,34,48] but significantly lower than experimental measurements,[49−51] which give approximately 75 kJ/(mol $H_2$), and highly accurate quantum Monte Carlo calculations,[52] which give $82 \pm 1$ kJ/(mol $H_2$) without vibrational contributions. If, in fact, the decomposition of $MgH_2$ occurs at higher temperatures than reaction (6*), the latter will be observable instead of reaction (5).

The $MgB_{12}H_{12}$ compound can be destabilized by mixing with $MgH_2$ according to reaction (7). Even though the gravimetric

(45) Chase, M. W., Jr.; Davies, C. A.; Downey, J. R., Jr.; Frurip, D. J.; McDonald, R. A.; Syverud, A. N. *J. Phys. Chem. Ref. Data* **1985**, *14*, 1.
(46) Reilly, J. J.; Wiswall, R. H. *Inorg. Chem.* **1967**, *6*, 2220–2223.
(47) Reilly, J. J.; Wiswall, R. H. *Inorg. Chem.* **1968**, *7*, 2254–2256.
(48) Hector, G. L.; Herbst, J. F. *Phys. Rev. B* **2007**, *76*, 014121.
(49) Stampfer, J. F.; Holley, C. E.; Suttle, J. F. *J. Am. Chem. Soc.* **1960**, *82*, 3504–3508.
(50) Bogdanovic, B.; Ritter, A.; Spliethoff, B. *Angew. Chem., Int. Ed. Engl.* **1990**, *29*, 223–234.
(51) Vajo, J. J.; Mertens, F.; Ahn, C. C.; Bowman, R. C.; Fultz, B. *J. Phys. Chem. B* **2004**, *108*, 13977–13983.
(52) Pozzo, M.; Alfè, D. *Phys. Rev. B* **2008**, *77*, 104103.

density of this reaction is acceptable (7.5 wt %), its thermodynamics are not useful for reversible on-board operation. It is interesting to note that destabilization of $MgB_{12}H_{12}$ with $CaH_2$ in a manner analogous to reaction (4) for $Li_2B_{12}H_{12}$ is not possible because an exothermic ion-exchange reaction leads to the formation of $CaB_{12}H_{12}$ and $MgH_2$. Finally, $CaB_{12}H_{12}$ can be destabilized by adding both $CaH_2$ and $MgH_2$ [reactions (8) and (9)]. The former route leads to a particularly dramatic effect, bringing the calculated decomposition temperature (86 °C) close to the upper limit of PEM fuel cells. Below we show that reactions (7) and (8) are involved in the thermodynamically preferred decomposition pathways of $Mg(BH_4)_2$ and $Ca(BH_4)_2$, respectively.

**Pure $LiBH_4$.** In agreement with ref 28, we find that lithium borohydride will decompose in a two-step process via an intermediate $Li_2B_{12}H_{12}$ compound, according to reactions (10) and (1) in Table 2. The first step (formation of $Li_2B_{12}H_{12}$) has an enthalpy of 44.4 kJ/mol $H_2$ and is predicted to occur at 171 °C when $p = 1$ bar, releasing 10 wt % hydrogen. In spite of the high hydrogen content, reaction (10) is not practically useful because its thermodynamics are incompatible with the operating temperatures of PEM fuel cells (80 °C). These results are in agreement with recent nuclear magnetic resonance (NMR) data,[30,31] which also indicate the presence of the $Li_2B_{12}H_{12}$ phase among the decomposition products of $LiBH_4$.

**Pure $Mg(BH_4)_2$.** We predict that magnesium borohydride also decomposes in a two-step sequence via an intermediate two-phase mixture of $MgB_{12}H_{12}$ and $MgH_2$.[29] While the first step, reaction (12), has rather good gravimetric storage capacity (8.1 wt %) and excellent thermodynamics (the predicted temperature of hydrogen release is 20 °C at $p = 1$ bar), the second decomposition step, reaction (7), is predicted to occur only at 128 °C, which is somewhat higher than the upper limit imposed by the PEM fuel cells. The decrease in the accessible gravimetric capacity relative to the intuitively appealing but thermodynamically unreasonable one-step reaction (13*) is rather dramatic and demonstrates that the existence of an intermediate $MgB_{12}H_{12}$ compound significantly decreases the attractiveness of pure $Mg(BH_4)_2$ for on-board hydrogen storage from the gravimetric capacity point of view, while at the same time improving the thermodynamics of partially dehydrogenating the material via reaction (12).

**Pure $Ca(BH_4)_2$.** Calcium borohydride is found to have two competing decomposition pathways with very similar thermodynamics. The calculated hydrogen release temperature for the one-step process via reaction (14) is the same (within numerical error) as the reaction temperatures for the two-step process involving an intermediate $CaB_{12}H_{12}$ phase via reactions (15) and (3). This suggests that all hydrogen might be extracted in one step, or at least in two steps with very similar thermodynamics. Calcium borohydride is predicted to have a very promising thermodynamic temperature of $H_2$ release just below 100 °C, though further destabilization of this compound would be beneficial.[22,23]

**Implications for the Stability of Borohydrides.** The above discussion shows that the existence of a stable intermediate, such as $X_nB_{12}H_{12}$, alters the reaction thermodynamics in such a way as to break up the decomposition into a portion that has a lower enthalpy than the "overall" decomposition and a portion that has a higher enthalpy. This is illustrated in Figure 3, which shows the total enthalpy of $LiBH_4$ and its decomposition products as a function of the number of $H_2$ molecules released. In this plot, the vertices correspond to stable states on the decomposition path, and the slopes of the line segments connecting these states give the corresponding reaction enthalpies. Figure 2 shows that, in the case of $LiBH_4$, the overall decomposition reaction (11*), $2LiBH_4 \rightarrow 2LiH + 2B + 3H_2$, with an enthalpy of ~65 kJ/mol $H_2$ and a temperature of 350 °C, is replaced by a sequence of two successive steps, $12LiBH_4 \rightarrow Li_2B_{12}H_{12} + 10LiH + 13H_2$ [reaction (10)] and $Li_2B_{12}H_{12} \rightarrow 2LiH + 12B + 5H_2$ [reaction (1)]. These two reactions have $T = 300$ K enthalpies of 44 and 117 kJ/mol $H_2$ and correspond to temperatures of 171 and 696 °C, respectively. Thus, the first stage occurs at a lower temperature, while the second stage occurs at a higher temperature than the overall one-step reaction (11*). Traditionally, $LiBH_4$ has been thought of as a material that is primarily limited by the poor thermodynamics of reaction (11*); therefore, various destabilization strategies have been proposed.[18−24] The present results show that the first decomposition step of $LiBH_4$ [reaction (10)] has better thermodynamics than previously thought, while the second step [reaction (1)] has extremely poor thermodynamics, much worse than previously thought. Since significant $H_2$ release from $LiBH_4$ is observed only above ~350 °C,[53] our results suggest that below these temperatures (but above ~170 °C) $LiBH_4$ is kinetically, not thermodynamically, limited. Likewise, for $Mg(BH_4)_2$ the desorption temperature for the commonly assumed one-step reaction (13*) should be 75 °C, while the formation of a $MgB_{12}H_{12}$ intermediate breaks this into a two-step process, where the first step occurs at 20 °C with $\Delta H^{300\ K} = 29.5$ kJ/(mol $H_2$), but the second step at a temperature of 128 °C with $\Delta H^{300\ K} = 50$ kJ/(mol $H_2$) is required to decompose $MgB_{12}H_{12}$. These results show that even though unexpectedly high temperatures are necessary to *fully* decompose $LiBH_4$ and $Mg(BH_4)_2$, a large fraction of the stored hydrogen can be extracted at lower temperatures than suggested by the commonly assumed one-step decomposition reactions (11*) and (13*).

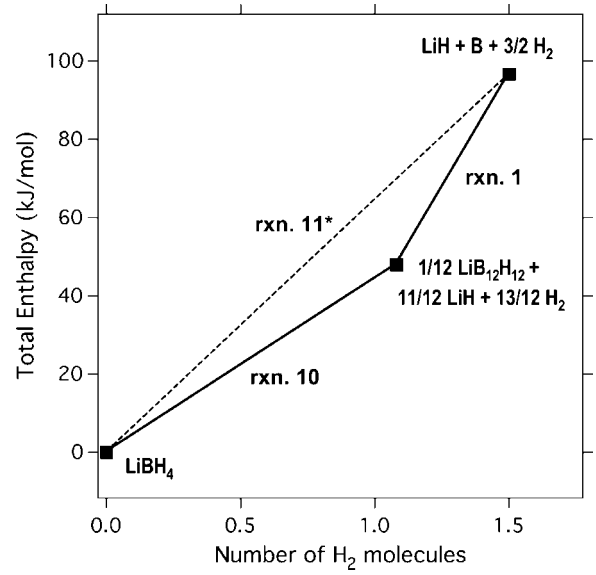


***Figure 3.*** Total $T = 300$ K enthalpy of $LiBH_4$ and its decomposition products for the predicted two-step process via reactions (10) and (1) in lieu of the one-step reaction (11*).

Having examined the predicted decomposition pathways and energetics of the individual borohydrides, we next turn to the

(53) Orimo, S.; Nakamori, Y.; Kitahara, G.; Miwa, K.; Ohba, N.; Towata, S.; Zuttel, A. *J. Alloys Compd.* **2005**, *404−406*, 427–430.

unique reactions that can occur via combinations of borohydrides and metal hydrides.

**D. Previously Proposed Borohydride Mixtures.** Our DFT results predict that the canonical destabilized reaction between $LiBH_4$ and $MgH_2$ proposed by Vajo et al.[18] [reaction (17*) in Table 2] is in fact a multistep process involving an intermediate $Li_2B_{12}H_{12}$ phase. Indeed, inspection of Table 2 shows that the decomposition of $LiBH_4$ into $Li_2B_{12}H_{12}$ via reaction (1) is favored to occur at lower temperatures than the one-step destabilized reaction (17*). Therefore, $Li_2B_{12}H_{12}$ will form first and subsequently decompose according to one of the destabilized reactions in Table 2 involving Mg or $MgH_2$:

$$12LiBH_4 + 6MgH_2 \rightarrow Li_2B_{12}H_{12} + 10LiH + 6MgH_2 + 13H_2$$
[reaction (10), $T_c = 171$ °C]

$$\rightarrow Li_2B_{12}H_{12} + 10LiH + 6Mg + 18H_2$$
[reaction (16), $T_c = 181$ °C]

$$\rightarrow 6MgB_2 + 12LiH + 24H_2$$ [reaction (5), $T_c = 259$ °C]

Due to the aforementioned tendency of the GGA to underestimate the decomposition temperature of $MgH_2$, it is likely that the latter remains stable up to the temperature of reaction (5) and the thermodynamic pathway is in fact a two-step sequence, as shown below:

$$12LiBH_4 + 6MgH_2 \rightarrow Li_2B_{12}H_{12} + 10LiH + 6MgH_2 + 13H_2$$
[reaction (10), $T_c = 171$ °C]

$$\rightarrow 6MgB_2 + 12LiH + 24H_2$$ [reaction (6*), $T_c = 215$ °C]

In both cases, $LiBH_4$ should first decompose into $Li_2B_{12}H_{12}$ according to reaction (1). Our theoretical results are consistent with recent experimental evidence for intermediate $Li_2B_{12}H_{12}$ compounds obtained using NMR measurements.[31]

It is interesting to note that the $Li_2B_{12}H_{12}$ compound does not have an effect on reaction (18) between $LiBH_4$ and $CaH_2$, which was first proposed by Alapati et al.[19] Reaction (18) is predicted to occur at 154 °C, slightly below the temperature where $LiBH_4$ decomposes into $Li_2B_{12}H_{12}$ via reaction (10). This observation suggests that, *to avoid the formation of intermediate $X_nB_{12}H_{12}$ phases, all properly designed destabilized borohydride reactions must have free energies that are lower than the free energies of reactions (10), (12), and (14).* This is a particular case of the guideline #1 formulated in ref 23.

**E. New Storage Reactions Involving Borohydride Mixtures.** We predict three new and previously unsuspected reactions, (19)−(21), belonging to a qualitatively new class of entropically optimized reactions that use fully hydrogenated high-entropy borohydrides as reactants and lead to the formation of low-entropy $X_nB_{12}H_{12}$ phases as end products. Two of these reactions, (19) and (20), possess nearly ideal thermodynamics, since they pass through the center of the target window for on-board storage in Figure 2. The first of these, reaction (19), uses a 5:2 molar mixture of Mg and Li borohydride, leading to the formation of $Li_2B_{12}H_{12}$ and $MgH_2$, accompanied by the release of 8.37 wt % $H_2$ at −29 °C and 1 bar $H_2$ pressure. The second reaction, (20), involves a 5:1 molar mixture of Mg and Ca borohydrides, leading to the formation $CaB_{12}H_{12}$ and $MgH_2$, releasing 7.73 wt % $H_2$ at −18 °C and 1 bar. Both reactions (19) and (20) have low enthalpies [~25 kJ/(mol $H_2$)], which should significantly simplify heat management during on-board recharging. Even though these enthalpy values are at the lower limit of the commonly accepted 20−45 kJ/(mol $H_2$) range, they are compatible with excellent thermodynamics due to the low vibrational entropies of the $Li_2B_{12}H_{12}$ and $CaB_{12}H_{12}$ product phases. They are an illustration of the above-formulated guideline for designing low-entropy reactions using product phases with large, tightly bound complex anions. These results demonstrate the power of the combined theoretical framework for structure prediction and linear programming-based reaction prediction, showing that previously unsuspected reactions can be found even in extensively studied materials systems.

The practical usefulness of these new reactions will be determined not only by their thermodynamics but also by the rate of hydrogen release, i.e., by their *kinetics*. Indeed, the dehydrogenation kinetics of $Mg(BH_4)_2$ have been measured: hydrogen desorption does not occur until very high temperatures, and the material has not been successfully rehydrided.[15,16,30] Our calculations clearly differentiate this type of thermodynamically preferred but kinetically limited reaction from the type that is thermodynamically limited. The former is an excellent candidate for enhanced reactivity via catalysis, whereas the latter is a dead-end and should be abandoned in the search for reversible solid-state storage systems. We note here an additional advantage of the new reactions (19) and (20) in comparison with some other previously proposed reactions.[22,23] The reaction products are $X_nB_{12}H_{12}$ compounds and $MgH_2$, while most of the known destabilized reactions [e.g., (17*) and (18)] lead to the formation of exceedingly stable metal borides, metal nitrides, or boron nitride as end products, which in practice serve as kinetic and thermodynamic "sinks".[24] Nevertheless, an effective catalyst will likely be needed to make the new reactions (19) and (20) practically useful.

## IV. Summary

We have demonstrated how a comprehensive first-principles framework involving DFT calculations of total energies and vibrational thermodynamics, new algorithms for crystal structure prediction, and linear programming-based determination of thermodynamically preferred reaction pathways can be used to shed new light on the existing hydrogen storage materials and predict completely new reactions with superior thermodynamic properties. We also propose a novel strategy of using reaction end products with large complex anions (such as $[B_{12}H_{12}]^{2-}$) to lower the entropies of hydrogen release from complex hydrides, which offers significant benefits by enabling the lowering of the optimal enthalpy range and therefore simplifying heat management during on-board recharging. In contrast to earlier studies, which only used information on known compounds, our work involves new intermediate phases with crystal structures that are not yet experimentally measured. This dramatically expands the range of the existing studies[22,23] by extending the realm of predictions from reactions with known compounds to reactions with new, currently unknown, and yet-to-be-synthesized materials. The proposed framework, possibly complemented by other methods for structure prediction (data mining,[44] genetic algorithms, etc.), should prove very useful for predicting new materials for other methods of energy storage, as long as they are based on phase transformations between different solid-state phases. This class of problems includes batteries and several other forms of electrochemical energy storage.[54]

**Acknowledgment.** The authors gratefully acknowledge financial support from the U.S. Department of Energy under grants DE-FG02-07ER46433 (V.O. and C.W.) and DE-AC04-94AL85000 (E.H.M.).

**Note Added in Proof.** After this paper was accepted, we became aware of a recent study by Her et al.,[55] which found a crystal structure of $Pa\bar{3}$ symmetry in solution-grown samples of $Li_2B_{12}H_{12}$. Our DFT calculations predict that the static $T = 0$ K energy of this structure is approximately 7 kJ/mol *higher* than that of the PEGS $C2/m$ structure found here. While further studies of structural polymorphism and vibrational free energies in $Li_2B_{12}H_{12}$ are clearly needed to explain the stability of the $Pa\bar{3}$ phase, the small energy difference between the $C2/m$ and $Pa\bar{3}$ structures will not qualitatively change any of the conclusions presented in this paper.

**Supporting Information Available:** Detailed information on the predicted crystal structures of $Li_2B_{12}H_{12}$, $MgB_{12}H_{12}$, and $CaB_{12}H_{12}$, including symmetries, inequivalent ionic positions, and ionic coordination. This material is available free of charge via the Internet at http://pubs.acs.org.

JA8066429

(54) Li, H.; Balaya, P.; Maier, J. *J. Electrochem. Soc.* **2004**, *151*, A1878–A1885.
(55) Her, J.-H.; Yousufuddin, M.; Zhou, W.; Jalisatgi, S. S.; Kulleck, J. G.; Zan, J. A.; Hwang, S.-J.; Bowman, R. C.; Udovic, T. J. *Inorg. Chem.* **2008**, *47*, 9757–9759.